2010 IEEE International Conference on Control Applications
Part of 2010 IEEE Multi-Conference on Systems and Control
Yokohama, Japan, September 8-10, 2010

Optimal amplitude quadrature control of an optical squeezer using an integral LQG approach

S. Z. Sayed Hassen and I. R. Petersen

***Abstract*— Squeezed states of light possess an asymmetric noise distribution whereby the uncertainty in one quadrature is less than the standard quantum noise limit. These states can be generated through a nonlinear optical process in an optical parametric oscillator (OPO). In this paper, we model such an optical squeezer and design an LQG controller which includes integral action to optimize the level of squeezing achieved in one of the quadratures of the fundamental optical field.**

I. Introduction

Nonlinear processes arising in quantum optics have proved useful in checking the counter-intuitive predictions of the theory of quantum mechanics. One of the simplest nonlinear optical processes, second harmonic generation (SHG), has been extensively studied and found to be a potential source of squeezed states of light. Squeezed light has an asymmetric quadrature noise distribution, with one quadrature having less noise than the standard quantum noise limit (SQL). This feature of squeezed states makes them particularly useful for applications such as gravitational wave detection (see [1]), where the use of squeezed light allows for a reduction of the laser power necessary to achieve a given signal to noise ratio. Other promising applications include quantum cryptography and optical communications. One of the main problems associated with the generation of squeezed states is due to what is known in the physics literature as "dephasing"; see [2]. Dephasing adds considerable phase noise to both the fundamental and second-harmonic fields inside an optical resonator cavity, and if unaccounted for, can completely destroy any squeezing achieved. This noise (also referred to as laser phase noise) occurs predominantly at low frequencies and can be modelled as a constant DC offset disturbance acting on the system.

In this paper, we address the problem of optimally squeezing a specific quadrature of light using an optimal parametric oscillator (OPO). We apply integral LQG control to an OPO driven by two optical fields $\hat{A}_{in}$ and $\hat{B}_{in}$; see Fig. 1. We include integral action as the standard LQG technique is not able to deal with the type of disturbance present in our application. One of the optical input fields ($\hat{B}_{in}$) is controlled by a mirror connected to a piezoelectric actuator. The actuator adjusts the phase quadrature of the optical field, thus minimizing the effect of phase noise and other classical sources of noise. This in turn regulates the phase angles of the fundamental and second-harmonic intra-cavity fields, allowing for squeezing of light in a spatial quadrature. The available measurement is the phase quadrature of the output second harmonic field $\hat{B}_{out}$ which is measured using the homodyne detection method; see [3]. One important feature of our approach is that we propose a control law that minimizes the noise in one quadrature of the fundamental output field using both measurement and actuation on the second harmonic field. The complete model we use for the controller design and subsequent simulations is derived from the linearized quantum dynamics of the OPO (optical subsystem) and from the model of a piezoelectric actuator (mechanical subsystem) typically found in a quantum optics laboratory.

A similar control design approach to the one presented here was investigated in [4] where the laser phase noise was modelled as (approximately) integrated white noise. Whilst this approximation of the phase noise was suitable for simulation purposes and to expose our ideas with regards to the specific problem, it turns out that the controller obtained in [4] is not appropriate in practice as it does not include integral action. Integral action is necessary to counteract any DC offset. The requirement to minimize the variance of the quadrature of the fundamental output field is reflected in an LQG cost functional and the need for integral action is included by modifying the control signals and the cost functional appropriately. Typical parameter values for an experimental squeezer are used for the controller design and we validate our design through simulation.

II. The Optical Parametric Amplification Problem

The optical system under consideration consists of a second-order nonlinear optical medium enclosed within an optical resonator [3]. Materials showing second-order nonlinearities $\chi^{(2)}$ have the ability to couple a fundamental field (f) to a second harmonic field ($2f$). This coupling forms the basis of operation of the OPO through nonlinear optical interaction and feedback resulting in the build-up of the waves in a process similar to that seen in a laser cavity. The output beams thus become quantum correlated producing squeezed light; ; see, e.g., [5], [6] for more details.

Fig. 1 shows our setup used for the OPO control problem. The aim is to maximize the amplitude quadrature squeezing of the fundamental optical field observed at a given operating point by optimally suppressing the different sources of noise feeding into the system. This aim is translated into a specific quadratic cost functional to define an LQG optimal control problem, the underlying assumption being that the

This work was supported by the Australian Research Council

S. Z. Sayed Hassen and I. R. Petersen are with the School of Engineering and Information Technology at the University of New South Wales, Canberra, ACT 2600, Australia. sayed.hassen@gmail.com

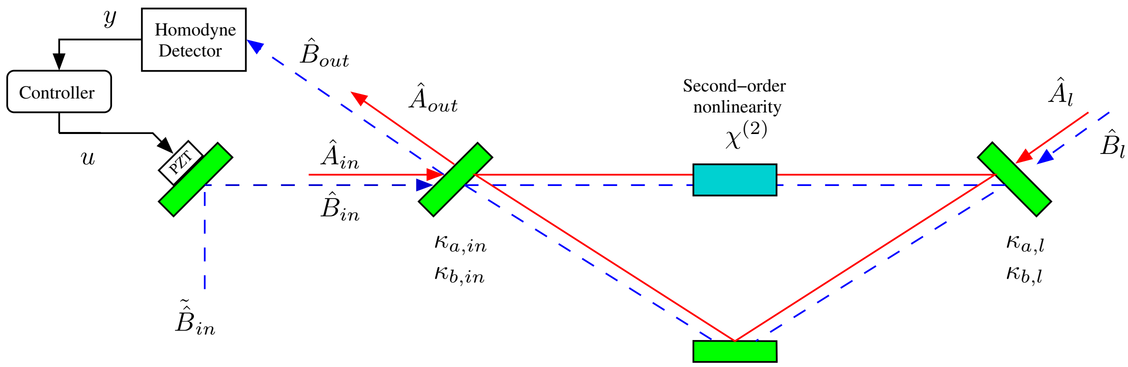

Fig. 1. Schematic for control of an optical parametric oscillator

conditional state associated with a quantum system can be equivalently modelled using a classical subsystem; see [7], [8], [9]. The measurement signal used is the phase quadrature of the second harmonic output field $\hat{B}_{out}$ which is measured using homodyne detection. The measured electrical signal is fed to a controller which determines the position of a mirror attached to a piezoelectric actuator, thus manipulating the phase quadrature of the input field $\hat{B}_{in}$ as desired.

III. Modelling

A. Optical Resonator Cavity

The dynamics of the OPO system is described in [4]. For completeness, we shall include it here as well (see also [3], [10]):

$$\dot{\hat{a}} = -\kappa_a \hat{a} + \chi^{(2)}\hat{a}^\dagger \hat{b} + \sqrt{2\kappa_{a,in}}\hat{A}_{in} + \sqrt{2\kappa_{a,l}}\delta\hat{A}_l; \quad (1)$$

$$\dot{\hat{b}} = -\kappa_b \hat{b} - \frac{1}{2}\chi^{(2)}\hat{a}^2 + \sqrt{2\kappa_{b,in}}\hat{B}_{in} + \sqrt{2\kappa_{b,l}}\delta\hat{B}_l; \quad (2)$$

where $a(a^\dagger)$ and $b(b^\dagger)$ are the annihilation (creation) operators for the fundamental and second harmonic fields respectively and $\kappa_{a,in}$ and $\kappa_{b,in}$ are the loss rates of the input/output mirrors for the $\hat{a}$ and $\hat{b}$ fields respectively. The parameters $\kappa_{a,l}$ and $\kappa_{b,l}$ are the internal loss rates for the corresponding two fields. Also, $\kappa_a = \kappa_{a,in} + \kappa_{a,l}$ and $\kappa_b = \kappa_{b,in} + \kappa_{b,l}$ are the associated total resonator decay rates. The quantities $\hat{A}_{in}$ and $\hat{B}_{in}$ are the input fields and $\delta\hat{A}_l$ and $\delta\hat{B}_l$ are the vacuum fields due to the internal losses. The output fields are given by:

$$\begin{aligned}\hat{A}_{out} &= \sqrt{2\kappa_{a,in}}\hat{a} - \hat{A}_{in};\\ \hat{B}_{out} &= \sqrt{2\kappa_{b,in}}\hat{b} - \hat{B}_{in}.\end{aligned}$$

B. Quadrature Operators

Quadrature operators provide a useful description of the properties of light and we shall use the amplitude quadrature and the phase quadrature (see [3]) defined as follows for the fields $\hat{a}$ and $\hat{b}$:

$$X_a^+ = \hat{a} + \hat{a}^\dagger; \qquad X_a^- = i(\hat{a}^\dagger - \hat{a}); \quad (3)$$

$$X_b^+ = \hat{b} + \hat{b}^\dagger; \qquad X_b^- = i(\hat{b}^\dagger - \hat{b}). \quad (4)$$

The quadratures of the input and noise fields can similarly be defined as $X_{Ain}^{\pm}, X_{Bin}^{\pm}, X_{\delta A,l}^{\pm}$ and $X_{\delta B,l}^{\pm}$. Then, the dynamics of the optical subsystem can be rewritten in terms of the quadratures as:

$$\begin{aligned}\dot{X}_a^+ &= -\kappa_a X_a^+ + \frac{1}{2}\chi^{(2)}(X_a^+X_b^+ + X_a^-X_b^-)\\ &\quad + \sqrt{2\kappa_{a,in}}X_{Ain}^+ + \sqrt{2\kappa_{a,l}}X_{\delta A,l}^+; \quad (5)\\ \dot{X}_a^- &= -\kappa_a X_a^- + \frac{1}{2}\chi^{(2)}(X_a^+X_b^- - X_a^-X_b^+)\\ &\quad + \sqrt{2\kappa_{a,in}}X_{Ain}^- + \sqrt{2\kappa_{a,l}}X_{\delta A,l}^-; \quad (6)\\ \dot{X}_b^+ &= -\kappa_b X_b^+ - \frac{1}{4}\chi^{(2)}({X_a^+}^2 - {X_a^-}^2)\\ &\quad + \sqrt{2\kappa_{b,in}}X_{Bin}^+ + \sqrt{2\kappa_{b,l}}X_{\delta B,l}^+; \quad (7)\\ \dot{X}_b^- &= -\kappa_b X_b^- - \frac{1}{2}\chi^{(2)}X_a^+X_a^-\\ &\quad + \sqrt{2\kappa_{b,in}}X_{Bin}^- + \sqrt{2\kappa_{b,l}}X_{\delta B,l}^-. \quad (8)\end{aligned}$$

The output fields are similarly expressed as

$$\begin{aligned}X_{Aout}^+ &= \sqrt{2\kappa_{a,in}}X_a^+ - X_{Ain}^+; \quad (9)\\ X_{Aout}^- &= \sqrt{2\kappa_{a,in}}X_a^- - X_{Ain}^-; \quad (10)\\ X_{Bout}^+ &= \sqrt{2\kappa_{b,in}}X_b^+ - X_{Bin}^+; \quad (11)\\ X_{Bout}^- &= \sqrt{2\kappa_{b,in}}X_b^- - X_{Bin}^-. \quad (12)\end{aligned}$$

C. Linearization

The dynamics of the optical subsystem (5)–(8) contain nonlinear terms and we use a standard linearization method to obtain linear dynamics to which we can apply LQG control design methods. To this end, we also determine the steady-state values $\bar{X}_i^{\pm}, i = a, b$, of the quadrature operators. The linearized dynamics of the optical subsystem is given by

$$\begin{aligned}\delta\dot{X}_a^+ &= -\kappa_a \delta X_a^+ + \frac{1}{2}\chi^{(2)}(\bar{X}_b^+\delta X_a^+ + \bar{X}_b^-\delta X_a^-\\ &\quad + \bar{X}_a^+\delta X_b^+ + \bar{X}_a^-\delta X_b^-)\\ &\quad + \sqrt{2\kappa_{a,in}}\delta X_{Ain}^+ + \sqrt{2\kappa_{a,l}}X_{\delta A,l}^+; \quad (13)\\ \delta\dot{X}_a^- &= -\kappa_a \delta X_a^- + \frac{1}{2}\chi^{(2)}(\bar{X}_b^-\delta X_a^+ - \bar{X}_b^+\delta X_a^-\\ &\quad - \bar{X}_a^-\delta X_b^+ + \bar{X}_a^+\delta X_b^-)\\ &\quad + \sqrt{2\kappa_{a,in}}\delta X_{Ain}^- + \sqrt{2\kappa_{a,l}}X_{\delta A,l}^-; \quad (14)\\ \delta\dot{X}_b^+ &= -\kappa_b \delta X_b^+ - \frac{1}{2}\chi^{(2)}(\bar{X}_a^+\delta X_a^+ - \bar{X}_a^-\delta X_a^-)\end{aligned}$$

$$+\sqrt{2\kappa_{b,in}}\delta X^{+}_{Bin} + \sqrt{2\kappa_{b,l}}X^{+}_{\delta B,l}; \quad (15)$$

$$\delta\dot{X}^{-}_{b} = -\kappa_b\delta X^{-}_{b} - \frac{1}{2}\chi^{(2)}(\bar{X}^{-}_{a}\delta X^{+}_{a} + \bar{X}^{+}_{a}\delta X^{-}_{a}) + \sqrt{2\kappa_{b,in}}\delta X^{-}_{Bin} + \sqrt{2\kappa_{b,l}}X^{-}_{\delta B,l}. \quad (16)$$

The corresponding linearized output fields are expressed as

$$\delta X^{+}_{Aout} = \sqrt{2\kappa_{a,in}}\delta X^{+}_{a} - \delta X^{+}_{Ain}; \quad (17)$$
$$\delta X^{-}_{Aout} = \sqrt{2\kappa_{a,in}}\delta X^{-}_{a} - \delta X^{-}_{Ain}; \quad (18)$$
$$\delta X^{+}_{Bout} = \sqrt{2\kappa_{b,in}}\delta X^{+}_{b} - \delta X^{+}_{Bin}; \quad (19)$$
$$\delta X^{-}_{Bout} = \sqrt{2\kappa_{b,in}}\delta X^{-}_{b} - \delta X^{-}_{Bin}. \quad (20)$$

D. *Optical parametric gain of the fundamental field $\hat{a}$*

In this section, we investigate the variation of the steady-state gain of the OPO under some specific conditions which are satisfied in our setup shown in Fig. 1. In particular, we determine the variation of the optical gain $|\hat{A}_{out}|^2/|\hat{A}_{in}|^2$ with respect to the quantities $\bar{\theta}_{a,in}$ and $\bar{\theta}_{b,in}$ (since energy is predominantly transferred from field $\hat{b}$ to $\hat{a}$). The relationship between them is shown in Fig. 2. The parameter values we use for our model are chosen to reflect those of a resonator cavity currently in operation in our laboratory. These values are as shown in Table I.

Model parameter	Value	Units
κ_a	1×10^5	rad/s
κ_b	1×10^9	rad/s
$\kappa_{a,l}$	5×10^3	rad/s
$\kappa_{b,l}$	5×10^7	rad/s
$\kappa_{a,in}$	9.5×10^4	rad/s
$\kappa_{b,in}$	9.5×10^8	rad/s
$\chi^{(2)}$	3×10^{-2}	–
$\bar{A}_{in}$	2×10^6	$\sqrt{\text{rad/s}}$
$\bar{B}_{in}$	2×10^{10}	$\sqrt{\text{rad/s}}$

TABLE I

MODEL PARAMETER VALUES

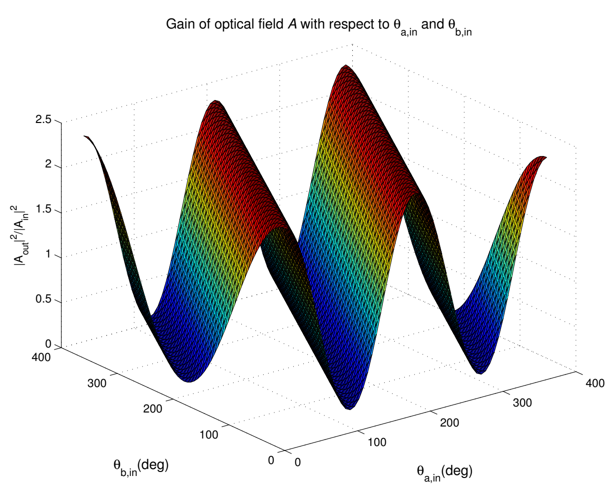

Fig. 2. Variation of the $|\hat{A}_{out}|^2/|\hat{A}_{in}|^2$ with $\bar{\theta}_{a,in}$ and $\bar{\theta}_{b,in}$

The variation of the gain $|\hat{A}_{out}|^2/|\hat{A}_{in}|^2$ with respect to the angles of the input fields, as shown in Fig. 2 is used in the determination of the operating point we would choose to obtain maximum squeezing. In particular, depending on the quadrature we would like to squeeze, we choose appropriate operating point(s) corresponding to a given pair of input field angles $\bar{\theta}_{a,in}$ and $\bar{\theta}_{b,in}$ such that we have the appropriate level of steady-state gain $|\hat{A}_{out}|^2/|\hat{A}_{in}|^2$.

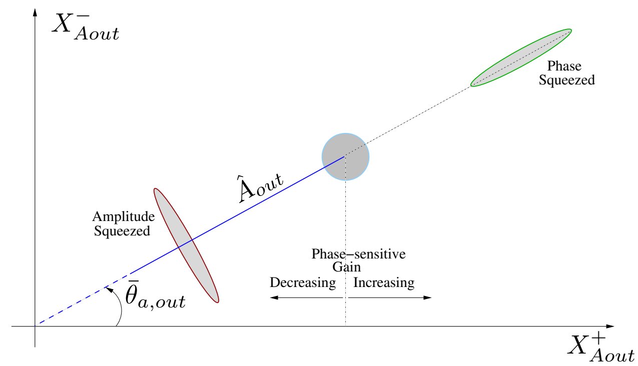

Fig. 3. Representation of phase sensitive squeezing

Fig. 3 illustrates the way in which we determine a type of squeezing and the extent of quadrature squeezing achieved. It shows the effect of varying the steady-state gain $|\hat{A}_{out}|^2/|\hat{A}_{in}|^2$ of a coherent state of light (minimum uncertainty state) denoted $\hat{A}_{out}$. The symmetric circular region represents the uncertainty associated with a given coherent state due to quantum noise. This noise is equally divided between the two quadratures. The figure shows how amplifying a quadrature by a given amount and de-amplifying the other quadrature by the same amount, a process which does not violate the quantum commutation relationships, results in a quadrature with an uncertainty level below the QNL. It should be emphasized that the gain here is provided by an OPO. Using our setup, we can thus change the noise distribution about the state from being circular and symmetric about the quadratures to elliptical and asymmetric. In particular, the noise variance along a given quadrature increases while that along the other quadrature decreases proportionately such that the Heisenberg uncertainty principle is not violated

$$\langle \delta X_{Aout}{}^{+2} \rangle \langle \delta X_{Aout}{}^{-2} \rangle \geq 1. \quad (21)$$

Here $\langle \cdot \rangle$ denotes the quantum expectation. Fig. 3 illustrates the idea that increasing the steady-state gain results in phase squeezing while decreasing the gain gives rise to amplitude squeezing. In our case, we are interested in maximizing the level of amplitude squeezing and we would therefore be ideally operating in a region where the optical steady-state gain is at its minimum. From Fig. 2, we can determine the required relationship between $\bar{\theta}_{a,in}$ and $\bar{\theta}_{b,in}$ in order that the optical gain is at its minimum. To achieve optimal amplitude squeezing, we would choose the operating point so that

$$\bar{\theta}_{b,in} - 2\bar{\theta}_{a,in} = n\pi; \quad \text{where } n \in \mathbb{Z}. \quad (22)$$

Furthermore, the relationship between $\bar{\theta}_{a,in}$ and $\bar{\theta}_a$ and between $\bar{\theta}_{b,in}$ and $\bar{\theta}_b$ can be determined from the nonlinear equations of the model described by (5)–(8). It can be shown that the phase of the applied input field $\bar{A}_{in}$ corresponds approximately to the phase of the field $\bar{a}$ inside the optical cavity. A similar correspondence exists between the phase of the input field $\bar{B}_{in}$ and the phase of the field $\bar{b}$ inside the optical cavity. Thus, an almost equivalent condition to (22) for maximum amplitude squeezing of the fundamental intracavity field $\hat{a}$ would be

$$\bar{\theta}_b - 2\bar{\theta}_a = n\pi. \tag{23}$$

E. Complete Model

We linearize the optical system about a set point defined by setting $\bar{A}_{in}$ and $\bar{B}_{in}$ so as to obtain a suitable pair $\bar{\theta}_a$ and $\bar{\theta}_b$ satisfying $\bar{\theta}_b - 2\bar{\theta}_a = \pi$. The results presented in Fig. 2 show that these values will lead to maximum observed amplitude quadrature squeezing of the field $\hat{A}$. One such pair could be $\bar{\theta}_a = \frac{\pi}{3}$ and $\bar{\theta}_b = \frac{5\pi}{3}$. Also, as stated above, the optical subsystem is controlled by regulating the phase quadrature of the second-harmonic input field (δX^-_{Bin}) using the phase quadrature of the second-harmonic output field (δX^-_{Bout}) as measurement.

We next model the piezo-actuator attached to the mirror (the mechanical subsystem) as a second order system:

$$\begin{aligned} \begin{bmatrix} \dot{\xi}_1 \\ \dot{\xi}_2 \end{bmatrix} &= \begin{bmatrix} 0 & 1 \\ -r_2 & -r_1 \end{bmatrix} \begin{bmatrix} \xi_1 \\ \xi_2 \end{bmatrix} + \begin{bmatrix} 0 \\ 1 \end{bmatrix} u; \\ \delta X^-_{Bin} &= \begin{bmatrix} c_2 & c_1 \end{bmatrix} \begin{bmatrix} \xi_1 \\ \xi_2 \end{bmatrix} + p_0. \end{aligned} \tag{24}$$

Here, ξ_1 represents deviation in the position of the mirror which controls the phase quadrature of the input field $\hat{B}_{in}(\delta X^-_{Bin})$. Also, p_0 represents the phase quadrature of the quantum noise present in the input field $\hat{B}_{in}$.

The complete linearized model can then be modelled in state-space form as:

$$\begin{aligned} \dot{x} &= Ax + B_1 u + B_2 w; \\ y &= Cx + Dw, \end{aligned} \tag{25}$$

where

$$\begin{aligned} x &= \begin{bmatrix} \delta X^+_a & \delta X^-_a & \delta X^+_b & \delta X^-_b & \xi_1 & \xi_2 & \xi \end{bmatrix}^T; \\ w &= \Big[\delta X^+_{Ain} \;\; \delta X^-_{Ain} \;\; \delta X^+_{Bin} \;\; p_0 \;\; X^+_{\delta A,l} \;\; X^-_{\delta A,l} \\ &\qquad\qquad X^+_{\delta B,l} \;\; X^-_{\delta B,l}\Big]^T. \end{aligned}$$

Fig. 4 shows the plant to be controlled. The quantity w_1 is used to represent laser phase noise which is modelled as a fixed DC offset feeding into the system for controller design purposes.

IV. LQG Integral Controller Design

A. Performance Criterion and Integral Action

The performance requirement for our control system is to minimize the variance of the amplitude quadrature of the output field $\hat{A}_{out}$, and to achieve squeezing in the presence

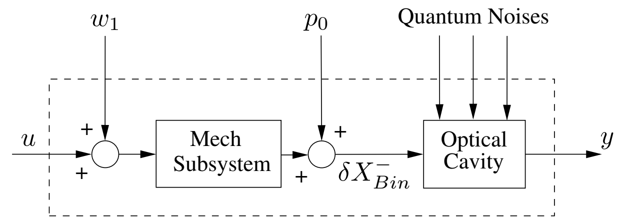

Fig. 4. Block diagram of system interconnections.

of both quantum and classical noises. The controlled variable is chosen such that the variations of the quadratures are measured along the direction of the steady-state output field, in particular along the phase angle $\bar{\theta}_{a,out}$. In general, an arbitrary quadrature, X^θ, can be described as a function of the phase angle θ, according to

$$X^\theta = X^+ \cos\theta + X^- \sin\theta. \tag{26}$$

Thus, to control the amplitude quadrature, we consider the controlled variable

$$z = \delta X^+_a \cos\bar{\theta}_{a,out} + \delta X^-_a \sin\bar{\theta}_{a,out}. \tag{27}$$

As shown in Fig. 4, our system is subjected to laser phase noise (w_1) which is most prominent at low frequencies, presenting itself as an initial DC offset acting on the system. Our application requires the elimination of those effects and standard LQG techniques will not provide satisfactory performance in the face of such a disturbance. This can be provided by including integral action in the LQG controller design process. To obtain a zero mean error value in the steady state due to the low frequency noise feeding into the system, we include integral action by adding an additional term in the cost function involving the integral of the controlled output. To this effect, we introduce the integral operator L, where

$$L(x) = \int_0^T A_2 x \, dt. \tag{28}$$

Here, A_2 is a constant matrix and is formed by selecting the state variables which are to be driven to zero in the steady-state. In our case, we choose

$$A_2 = \begin{bmatrix} \cos\bar{\theta}_{a,out} & \sin\bar{\theta}_{a,out} & 0 & 0 & 0 & 0 & 0 \end{bmatrix},$$

so that $z = A_2 x$.

The integral LQG performance criterion can then be formulated as the minimization of the following cost function:

$$\mathcal{J} = \lim_{T\to\infty} \mathbf{E}\left[\frac{1}{T}\int_0^T x'Q_1 x + L(x)'Q_2 L(x) + u'Ru \, dt\right]. \tag{29}$$

We choose the matrices Q_1, Q_2 and R such that

$$x'Q_1x = |z|^2, \; u'Ru = r|u|^2, \; Q_2 = q_2; \tag{30}$$

where q_2, $r > 0$ are treated as design parameters. The expectation in (29) is with respect to the Gaussian quantum and classical noise processes, and the assumed Gaussian initial conditions. Fig. 5 shows the setup used for the integral LQG

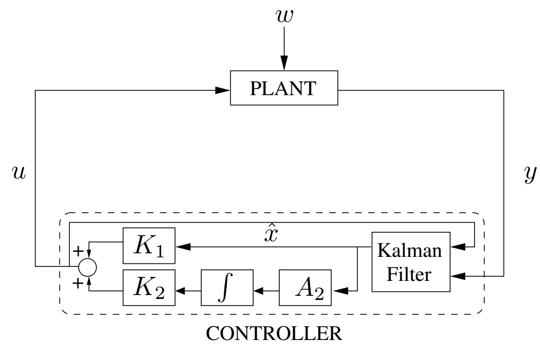

Fig. 5. Integral LQG controller design configuration.

controller design. The integral LQG controller is formed by combining the Kalman filter with the optimal state feedback control law K_1 and K_2 in the integrator path; see Fig. 5. This controller would then satisfy the specified performance requirements as described above. To apply standard LQG result, the problem is transformed by augmenting the state variables of the system as follows. We define

$$\tilde{x} = \begin{bmatrix} x \\ L(x) \end{bmatrix}; \tag{31}$$

and we rewrite the state equations as

$$\begin{aligned} \dot{\tilde{x}} &= \tilde{A}\tilde{x} + \tilde{B}_1 u + \tilde{B}_2 w; \\ y &= \tilde{C}\tilde{x} + Dw, \end{aligned}$$

where

$$\tilde{A} = \begin{bmatrix} A & 0 \\ A_2 & 0 \end{bmatrix}; \; \tilde{B}_1 = \begin{bmatrix} B_1 \\ 0 \end{bmatrix}; \; \tilde{B}_2 = \begin{bmatrix} B_2 \\ 0 \end{bmatrix}; \quad \tilde{C} = \begin{bmatrix} C & 0 \end{bmatrix}. \tag{32}$$

The performance criterion is then reformulated as

$$\mathcal{J} = \lim_{T\to\infty} \mathbf{E}\left[\frac{1}{T}\int_0^T \tilde{x}'\bar{Q}\tilde{x} + u'Ru \, dt\right], \tag{33}$$

where

$$\bar{Q} = \begin{bmatrix} Q_1 & 0 \\ 0 & Q_2 \end{bmatrix}. \tag{34}$$

The LQG optimal controller is constructed from the solution to a deterministic regulator problem and an optimal observer problem as follows (e.g., see [11], [12]):

$$\begin{aligned} u &= -K\hat{\tilde{x}} \\ &= -K_1\hat{x} - K_2 L(\hat{x}). \end{aligned} \tag{35}$$

The optimal feedback gain matrix is given by

$$\begin{aligned} K &= [K_1 \;\; K_2] \\ &= r^{-1}\tilde{B}_1^T X, \end{aligned} \tag{36}$$

where X satisfies the matrix Riccati equation:

$$\bar{Q} - r^{-1}X\tilde{B}_1\tilde{B}_1^T X + X\tilde{A} + \tilde{A}^T X = 0. \tag{37}$$

The optimal observer dynamics (Kalman filter) are described by

$$d\hat{\tilde{x}} = \tilde{A}\hat{\tilde{x}}\,dt + \tilde{B}_1 u\,dt + L[dy - \tilde{C}\hat{\tilde{x}}\,dt]; \tag{38}$$

and the solution of the optimal observer is obtained by choosing the gain matrix

$$L = (P_e\tilde{C}^T + \tilde{B}_2 D^T)(DD^T)^{-1}, \tag{39}$$

where P_e is the solution to the matrix Riccati equation

$$\begin{aligned} &(\tilde{A} - \tilde{B}_2 D^T(DD^T)^{-1}\tilde{C})P_e \\ &+ \;\; P_e(\tilde{A} - \tilde{B}_2 D^T(DD^T)^{-1}\tilde{C})^T \\ &- \;\; P_e\tilde{C}^T(DD^T)^{-1}\tilde{C}P_e + \tilde{B}_2\tilde{B}_2^T \\ &- \;\; B_2 D^T(DD^T)^{-1}D\tilde{B}_2^T = 0. \end{aligned} \tag{40}$$

B. Model and Design Parameters

The parameter values of the piezoelectric actuator and the steady-state phase angles of the input fields are shown in Table II.

Model parameter	Value
r_1	1×10^4
r_2	1×10^9
c_1	-5×10^3
c_2	1.5×10^{10}
$\bar{\theta}_{a,in}$	$\pi/3$
$\bar{\theta}_{b,in}$	$5\pi/3$

TABLE II
MODEL PARAMETERS

In designing the LQG controller, the design parameters ϵ_1^2 (quantum noise variance), ϵ_2^2 (sensor noise variance), R (the control energy weighting in the cost functional) and Q_2 were adjusted until good performance was obtained in the controller simulations. The values used were $\epsilon_1 = 1 \times 10^{-3}$, $\epsilon_2 = 1 \times 10^{-5}$, $R = 3.2 \times 10^{-7}$ and $Q_2 = 4 \times 10^{15}$. The large value of Q_2 is chosen to enforce integral action. These parameters led to an LQG controller and the corresponding loop gain Bode plot is shown in Fig. 6. This plot shows that we have high gain at low frequencies where the slowly varying phase noise predominates and that due to the integral action, we have infinite gain at DC to cater for the constant disturbance present in our application.

V. SIMULATION RESULTS

Using the model parameters specified in Tables I and II, we simulate the closed-loop system to demonstrate the effectiveness of the controller using SIMULINK®. We consider the case where the system is excited with both classical and quantum noises. Fig. 7 shows the laser phase noise w_1, modelled as integrated white noise superimposed over a fixed DC offset. The corresponding control signal u generated by the controller is also shown.

The movement of the mirror compensating for the laser phase noise is shown in Fig. 8 and finally, Fig. 9 shows the time history of the uncontrolled and controlled variable z.

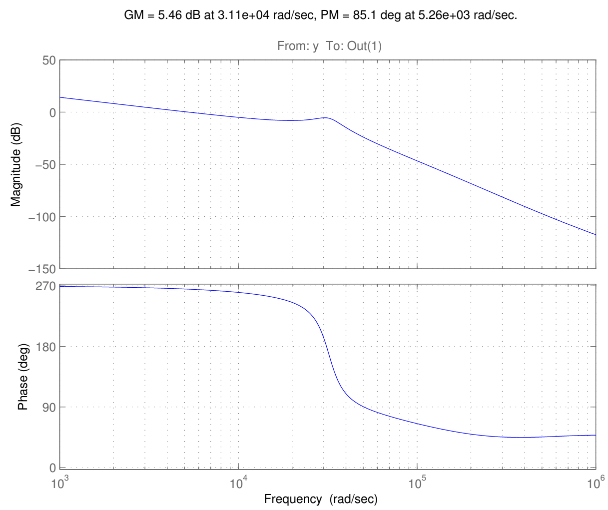

Fig. 6. Bode plot of loop gain transfer function

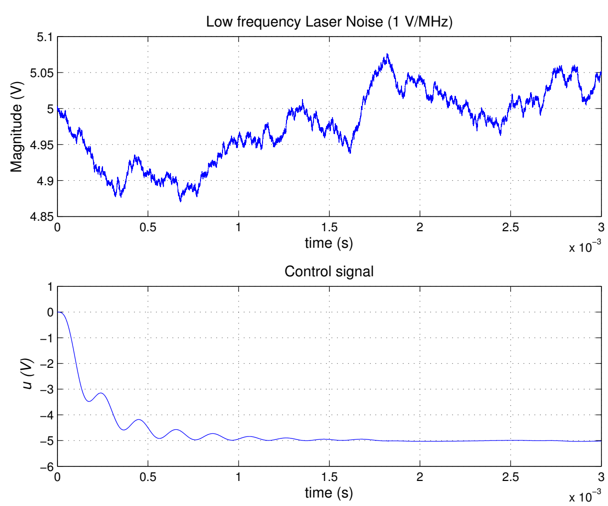

Fig. 7. Laser phase noise w_1 and control signal u

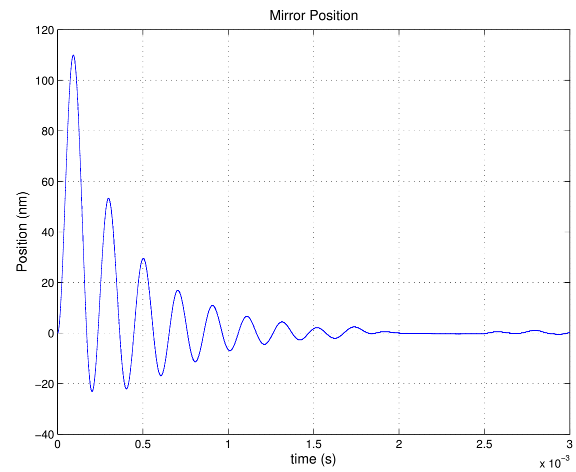

Fig. 8. Mirror movement

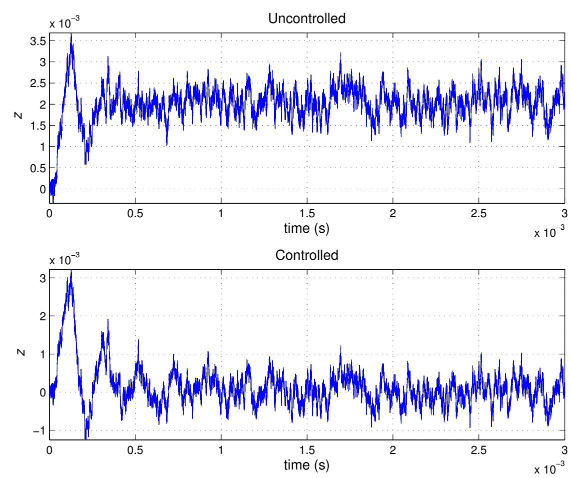

Fig. 9. The uncontrolled and controlled variable z

VI. Conclusion and Future Work

An integral LQG controller was designed to optimize the level of squeezing achieved in an optical squeezer. A non-linear model of an optical parametric oscillator was derived and steady-state conditions required to achieve maximum amplitude quadrature squeezing of the fundamental field were calculated. At a suitable operating point, the system was linearized and an optimal state feedback control law was determined from a given cost functional. The cost functional was chosen to reflect our goal of minimizing the variance of the amplitude quadrature of the fundamental output field. Simulation results obtained show the effectiveness of the controller in cancelling out the laser phase noise and that the control system performance becomes limited only by quantum noises. The next stage of our work will involve implementation of this controller on an experimental test-bed.

References

[1] C. M. Caves, "Quantum-mechanical noise in an interferometer," *Phys. Rev. D*, vol. 23, no. 8, pp. 1693–1708, Apr 1981.
[2] A. E. Siegman, *Lasers*. University Science Books, 1986.
[3] H. A. Bachor and T. C. Ralph, *A Guide to Experiments in Quantum Optics*. John Wiley, 2004.
[4] S. Z. Sayed Hassen, I. R. Petersen, E. H. Huntington, M. Heurs, and M. R. James, "LQG control of an optical squeezer," in *Proc. American Control Conf.*, Baltimore, Maryland, US, July 2010, Accepted.
[5] R. W. Boyd, *Nonlinear Optics*. Academic Press, Boston, 2008.
[6] C. W. Gardiner and P. Zoller, *Quantum Noise*. Springer, Berlin, 2000.
[7] S. C. Edwards and V. P. Belavkin, "Optimal quantum feedback control via quantum dynamic programming," 2005, arXiv:quant-ph/0506018.
[8] K. Jacobs, "Applications of feedback control in quantum systems," in *Proc. 6th Asian Cont. Conf.*, 2006, p. 35, quant-ph/0605015.
[9] A. C. Doherty and K. Jacobs, "Feedback control of quantum systems using continuous state estimation," *Phys. Rev. A*, vol. 60, no. 2700, 1999.
[10] N. Hodgson and H. Weber, *Laser Resonators and Beam Propagation*, ser. Optical Sciences. Springer Science, 2005.
[11] H. Kwakernaak and R. Sivan, *Linear Optimal Control Systems*. John Wiley & Sons, Inc., 1972.
[12] M. J. Grimble, "Design of optimal stochastic regulating systems including integral action," *Proc. IEE Control & Science*, vol. 126, no. 9, pp. 841–848, Sept. 1979.